Lightning Current Waveforms Inferred From Far-Field Waveforms for the Case of Strikes to Tall Objects

Shunsuke Koike, Yoshihiro Baba¹⁰, Fellow, IEEE, Toshihiro Tsuboi, and Vladimir A. Rakov¹⁰, Fellow, IEEE

Abstract—Electric and magnetic fields at far distances produced by lightning strikes to tall objects are different from those associated with lightning strikes to flat ground. Specifically, in the case of strikes to tall objects, the waveforms are oscillatory because of current reflections at the top and bottom of the tall object. In this article, a procedure to reconstruct the waveform of far electric field due to the lightning strike to flat ground from the corresponding waveform of far electric field due to a lightning strike to a tall object is proposed. Once the effect of tall strike object is removed from the measured field waveform, the channel-base current for the strike to flat ground is estimated. Further, the channel-base current waveform is used to find the waveform of current at any altitude along both the strike object and the lightning channel. Computations of far electric fields due to lightning strikes to tall objects are carried out using the finite-difference time-domain method in the two-dimensional cylindrical coordinate system. The lightning return stroke is represented by the transmission-line (TL) model, the modified TL model with linear current decay with height, or the modified TL model with exponential current decay with height.

Index Terms—Finite-difference time-domain (FDTD) method, lightning, return-stroke current waveform, return-stroke field waveform, return-stroke model, tall object.

I. INTRODUCTION

ALL objects are often struck by lightning [1], [2], [3]. Electric and magnetic fields produced at far distances by lightning strikes to tall objects are different from those associated with lightning strikes to flat ground. Specifically, in the case of strikes to tall objects, the waveforms are oscillatory because of current reflections at the top and bottom of the tall object. It would be of great scientific interest and practical use if the distribution of lightning current both along the channel and along the strike object could be estimated from measured waveforms of far electric or magnetic field.

Manuscript received 11 February 2023; revised 17 March 2023; accepted 22 March 2023. Date of publication 17 April 2023; date of current version 15 August 2023. This work was supported by the U.S. National Science Foundation under Grant AGS-2055178. (Corresponding author: Yoshihiro Baba.)

Shunsuke Koike and Yoshihiro Baba are with the Doshisha University, Kyoto 610-0394, Japan (e-mail: ctwg0314@mail4.doshisha.ac.jp; ybaba@mail.doshisha.ac.jp).

Toshihiro Tsuboi is with the TEPCO Research Institute, Kanagawa 230-0002, Japan (e-mail: tsuboi.toshihiro@tepco.co.jp).

Vladimir A. Rakov is with the Department of Electrical and Computer Engineering, University of Florida, Gainesville, FL 32611 USA (e-mail: rakov@ece.ufl.edu).

Color versions of one or more figures in this article are available at https://doi.org/10.1109/TEMC.2023.3261422.

Digital Object Identifier 10.1109/TEMC.2023.3261422

In this article, a procedure to reconstruct the waveform of far electric field due to the lightning strike to flat ground from the corresponding waveform of far electric field due to a lightning strike to a tall object is proposed. Then, the waveform of channel-base current for the strike to flat ground is estimated using the procedure proposed by Fukuyama et al. [4]. Further, the channel-base current waveform is used to find the waveform of current at any altitude along either the strike object or the lightning channel using the expressions proposed by Baba and Rakov [5]. Computations of far electric fields due to lightning strikes to tall objects are carried out using the finite-difference time-domain (FDTD) method [6] in the two-dimensional (2-D) cylindrical coordinate system. The lightning return stroke is represented by the transmission-line (TL) model [7], the modified TL model with linear current decay with height (MTLL) [8], or the modified TL model with exponential current decay with height (MTLE) [9].

II. SPATIAL AND TEMPORAL DISTRIBUTIONS OF CURRENT ALONG A TALL STRIKE OBJECT AND A LIGHTNING CHANNEL

Current I(z', t) at an arbitrary height z' along a tall strike object of height h and along the lightning channel attached to the object top at arbitrary time t, based on their TL representation, is given by (6a) and (6b) of [5], which are as follows (see also Fig. 1(b) in [5]):

$$I\left(z',t\right) = \frac{1 - \rho_{\text{top}}}{2} \sum_{n=0}^{\infty} \begin{bmatrix} \rho_{\text{bot}}^{n} \rho_{\text{top}}^{n} I_{\text{sc}} \left(h, t - \frac{h - z'}{c} - \frac{2nh}{c}\right) \\ + \rho_{\text{bot}}^{n+1} \rho_{\text{top}}^{n} I_{\text{sc}} \left(h, t - \frac{h + z'}{c} - \frac{2nh}{c}\right) \end{bmatrix}$$
(1a)

for $0 \le z' < h$ (tall object) and

$$I(z',t) = \frac{1 - \rho_{\text{top}}}{2}$$

$$\times \left[I_{\text{sc}} \left(h, t - \frac{z' - h}{v} \right) + (1 + \rho_{\text{top}}) \sum_{n=1}^{\infty} \rho_{\text{bot}}^{n} \rho_{\text{top}}^{n-1} I_{\text{sc}} \left(h, t - \frac{z' - h}{v} - \frac{2nh}{c} \right) \right]$$

$$\times u \left(t - \frac{z' - h}{v_f} \right)$$

$$(1b)$$

for $z' \geq h$ (lightning channel), where $I_{\rm sc}$ is the lightning short-circuit current that is defined as the lightning current that would be measured at an ideally grounded object ($Z_{\rm gr}=0$ or $Z_{\rm gr}<< Z_{\rm ch}$) of negligible height, $\rho_{\rm bot}$ is the current reflection coefficient

0018-9375 © 2023 IEEE. Personal use is permitted, but republication/redistribution requires IEEE permission. See https://www.ieee.org/publications/rights/index.html for more information.

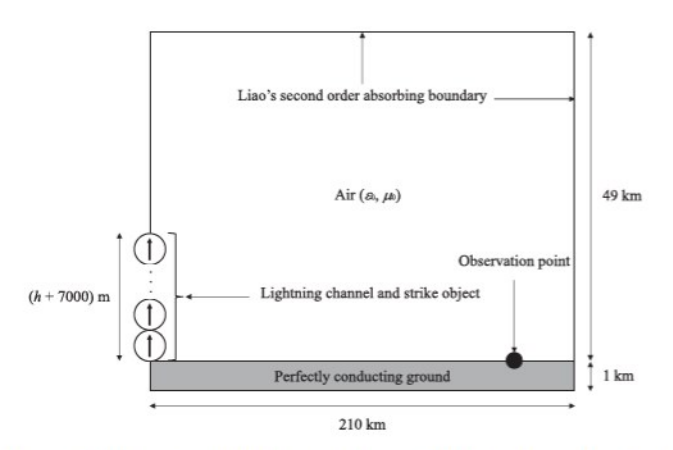


Fig. 1. Configuration of a lightning strike to a tall object to be analyzed with the FDTD method in the 2-D cylindrical coordinate system.

at the bottom of strike object, $\rho_{\rm top}$ is the current reflection coefficient at the object top for current waves propagating upward, n is an index representing the successive multiple reflections occurring at the two ends of the strike object, c is the speed of light, v_f is the return-stroke wavefront speed, v is the current propagation speed along the lightning channel, and u is the Heaviside unit function. If the grounding impedance is $Z_{\rm gr}$, the characteristic impedance of the tall object is $Z_{\rm ob}$, the equivalent impedance of the lightning return-stroke channel is Z_c , then the current reflection coefficients are given by $\rho_{\rm bot} = (Z_{\rm ob} - Z_{\rm gr})/(Z_{\rm ob} + Z_{\rm gr})$ and $\rho_{\rm top} = (Z_{\rm ob} - Z_{\rm ch})/(Z_{\rm ob} + Z_{\rm ch})$.

The spatial and temporal distribution of current along a lightning channel terminated on flat ground ($z' \ge 0$), based on the TL representation [5], is given as follows:

$$I(z', t) = \frac{1 + \rho_{gr}}{2} I_{sc} \left(0, t - \frac{z'}{v}\right)$$
 (2)

where $\rho_{\rm gr}$ is the current reflection coefficient at the lightning channel base, which is given by $\rho_{\rm gr} = (Z_{\rm ch} - Z_{\rm gr})/(Z_{\rm ch} + Z_{\rm gr})$.

Equations (1b) and (2) are expressions for a lightning channel represented by the TL model. If lightning channel is represented by the MTLL model, (1b) needs to be multiplied by [1-(z'-h)/H] and (2) needs to be multiplied by (1-z'/H), where H is the total channel length in the MTLL model. If lightning channel is represented by the MTLE model, (1b) needs to be multiplied by $\exp[-(z'-h)/\lambda]$ and (2) needs to be multiplied by $\exp[-(z'-h)/\lambda]$, where λ is the current decay height constant.

III. FDTD COMPUTATIONS OF FAR FIELDS DUE TO LIGHTNING STRIKES TO TALL OBJECTS

Fig. 1 shows the configuration of a lightning strike to a tall object to be analyzed using the FDTD method in the 2-D cylindrical coordinate system. In this coordinate system, there exist only the radial and vertical components of electric field, E_{τ} and E_z , respectively, and the azimuthal component of magnetic field, H_{φ} . Time-update equations for E_{τ} , E_z , and H_{φ} are given in Appendix. The computational domain is 210 km \times 50 km, which is divided uniformly into rectangular cells of 5 m \times 10 m. The time increment is set to 14.8 ns. Liao's second-order absorbing boundary condition [10] is applied to all sides of the computational domain except for its left side. The

ground is set to be perfectly conducting. The tall strike object and the 7-km long lightning channel are located at the left-side boundary of the 2-D computational domain. The spatial and temporal distributions of current along the tall strike object and the lightning channel given by (1a) and (1b), respectively, or by (2) in the absence of strike object, are represented by a vertical current source array [11].

The total channel length in the MTLL model is set to H = 7km, and the current decay height constant in the MTLE model is set to $\lambda = 2$ km. The current propagation speed v along the lightning channel and the return-stroke wavefront speed v_f are both set to 150 m/ μ s (0.5c). The waveform of the short-circuit current I_{sc} is represented by the sum of a Heidler function [12] and a double-exponential function, so that its peak is 11 kA and the risetime is 1 μ s. The grounding impedance is set to $Z_{gr} =$ 10 Ω and the equivalent impedance of lightning channel is set to $Z_{ch} = 1000 \Omega$. Therefore, the current reflection coefficient at the base of the lightning channel attached to flat ground is $\rho_{\rm gr} =$ $(Z_{ch} - Z_{gr})/(Z_{ch} + Z_{gr}) = 0.98$, and the peak of the channel-base current is $(1 + \rho_{gr})/2 \times I_{sc} = (1 + 0.98)/2 \times 11 \text{ kA} = 10.9 \text{ kA}$. The characteristic impedance of the strike object is set to $Z_{ob} =$ 250 Ω , so that current reflection coefficients at the bottom and top of strike object are $\rho_{\rm bot} = (Z_{\rm ob} - Z_{\rm gr})/(Z_{\rm ob} + Z_{\rm gr}) = 0.92$ and $\rho_{\text{top}} = (Z_{\text{ob}} - Z_{\text{ch}})/(Z_{\text{ob}} + Z_{\text{ch}}) = -0.6$.

Fig. 2 shows FDTD-computed waveforms of electric field due to lightning strikes to 200, 300, 400, and 500-m tall objects and to flat ground at a distance of 200 km from the lightning channel for the TL, MTLL, and MTLE models. Waveforms of electric field associated with a lightning strike to a tall object exhibit oscillations due to successive reflections of lightning current at the top and bottom of the strike object. This is in contrast with the waveforms for the case of lightning strike to flat ground, which exhibit no oscillations. Also, peaks of electric field associated with lightning strikes to tall objects are greater than those associated with lightning strike to flat ground for reasons discussed in [13] and [14].

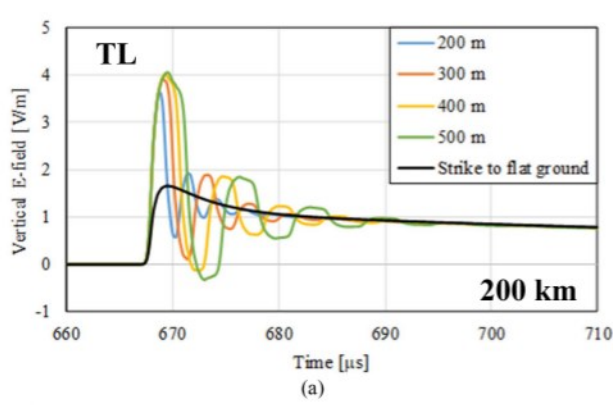
Peak values of electric field due to the corresponding lightning strike to flat ground, computed using the TL, MTLL, and MTLE models, are 1.65, 1.61, and 1.51 V/m, respectively. The ratio of electric-field peaks of lightning strikes to the tall object and to flat ground ranges from 2.20 to 2.45 for the TL model, from 2.25 to 2.49 for the MTLL model, and from 2.36 to 2.60 for the MTLE model.

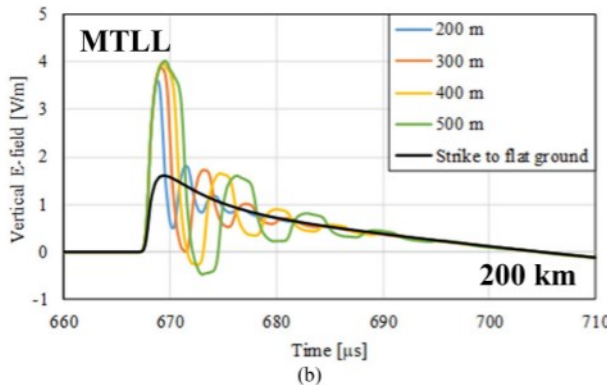
Baba and Rakov [13] have derived the following expression for the far-field-enhancement factor k_{tall} due to the presence of tall strike object:

$$k_{\text{tall}} = \frac{(v+c)(1-\rho_{\text{top}})}{v(1+\rho_{\text{er}})}.$$
 (3)

This expression yields $k_{\rm tall} = 2.4$, for v = 0.5c, $\rho_{\rm top} = -0.6$, and $\rho_{\rm gr} = 0.98$, which is close to the above-given field-peak ratios based on the FDTD computations.

Table I gives values of the first maximum $E_{z_{\rm tall.max}}$ and the first minimum $E_{z_{\rm tall.min}}$ of vertical electric field for 200, 300, 400, and 500-m tall objects computed with the TL model.





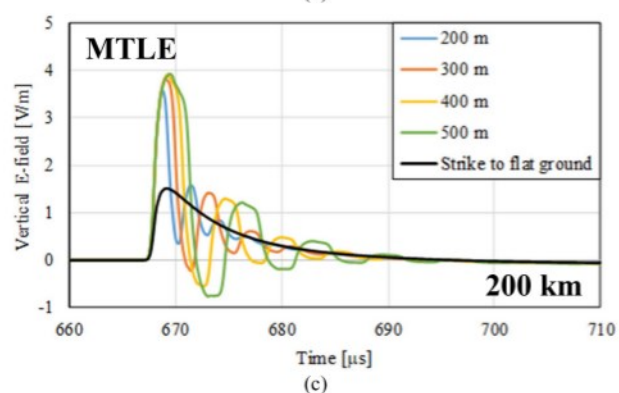


Fig. 2. FDTD-computed waveforms of electric field due to lightning strikes to 200, 300, 400, and 500-m tall objects and to flat ground at a distance of 200 km from the lightning channel for (a) TL model, (b) MTLL model, and (c) MTLE model.

TABLE I

VALUES OF THE FIRST MAXIMUM $E_{\rm Z_TALL.MAX}$ AND THE FIRST MINIMUM $E_{\rm Z_TALL.MIN}$ OF VERTICAL ELECTRIC FIELD DUE TO LIGHTNING STRIKES TO 200, 300, 400, AND 500-M TALL OBJECTS AT A DISTANCE OF 200 KM FROM THE LIGHTNING CHANNEL, COMPUTED WITH THE TL MODEL

h [m]	200	300	400	500
$E_{z tall.max}$ [V/m]	3.63	3.91	4.01	4.04
Ez tall.min [V/m]	0.57	0.11	-0.12	-0.33

Similarly, Table II gives those computed with the MTLL model, and Table III gives those computed with the MTLE model. The first maximum and first minimum field values will be used in the procedure to reconstruct the waveform of far electric field due to the lightning strike to flat ground from the corresponding waveform of far electric field due to lightning strikes to tall objects, which is discussed in Section IV.

TABLE II
VALUES OF $E_{z_TALL.MAX}$ AND $E_{z_TALL.MIN}$ OF VERTICAL ELECTRIC FIELD

h [m]	200	300	400	500
Ez tall.max [V/m]	3.62	3.89	3.98	4.01
E- tall min [V/m]	0.50	0.01	-0.27	-0.48

COMPUTED WITH THE MTLL MODEL

TABLE III

VALUES OF $E_{z_TALL.MAX}$ AND $E_{z_TALL.MIN}$ OF VERTICAL ELECTRIC FIELD

COMPUTED WITH THE MTLE MODEL

h [m]	200	300	400	500
$E_{z \ tall.max} [V/m]$	3.57	3.82	3.90	3.92
Ez tall.min [V/m]	0.35	-0.22	-0.55	-0.77

IV. PROPOSED PROCEDURE FOR RECONSTRUCTION OF THE WAVEFORM OF ELECTRIC FIELD DUE TO THE CORRESPONDING LIGHTNING STRIKE TO FLAT GROUND

From (1a), the currents at the bottom of strike object (z' = 0) at times t and t-2h/c are given as follows:

$$\begin{split} I\left(0,t\right) &= \frac{(1+\rho_{\text{bot}})(1-\rho_{\text{top}})}{2} \\ &\times \left\{ I_{\text{sc}}\left(h,t-\frac{h}{c}\right) + \sum_{n=1}^{\infty} \left[\rho_{\text{bot}}^{n} \rho_{\text{top}}^{n} I_{\text{sc}}\left(h,t-\frac{2(n+1)h}{c}\right) \right] \right\} \end{split} \tag{4}$$

$$I\left(0, t - \frac{2h}{c}\right) = \frac{\left(1 + \rho_{\text{bot}}\right)\left(1 - \rho_{\text{top}}\right)}{2\rho_{\text{bot}}\rho_{\text{top}}}$$
$$\times \sum_{n=1}^{\infty} \left[\rho_{\text{bot}}^{n}\rho_{\text{top}}^{n}I_{\text{sc}}\left(h, t - \frac{2\left(n+1\right)h}{c}\right)\right]. \quad (5)$$

It appears from (4) and (5) that the short-circuit current $I_{\rm sc}$ (h, t-h/c) at height z'=h and at time t-h/c can be expressed using currents at the bottom of the strike object I(0, t) and I(0, t-2h/c) at times t and t-2h/c. Indeed, combining (4) and (5) to eliminate $\sum \rho^n_{\rm bot} \rho^n_{\rm top} I_{\rm sc} (h, t-2(n+1)h/c)$, we obtain

$$\begin{split} I_{\text{sc}}\left(h,t-\frac{h}{c}\right) &= \frac{2}{\left(1+\rho_{\text{bot}}\right)\left(1-\rho_{\text{top}}\right)} \\ &\times \left[I\left(0,t\right)-\rho_{\text{bot}}\rho_{\text{top}}I\left(0,t-\frac{2h}{c}\right)\right]. \end{split} \tag{6}$$

If currents I(0, t) and I(0, t - 2h/c) at the bottom of strike object on the right-hand side of (6) were replaced by vertical electric fields due to a lightning strike to a tall object, E_{z_tall} (0, t) and E_{z_tall} (0, t - 2h/c), respectively, as done in (7), the waivetail of the resultant E_z waveform (from about 15 to 45 μ s) would agree well with that of the electric field due to the corresponding lightning strike to flat ground. This is illustrated in Fig. 3 for h = 500 m, where the flat-ground waveform is plotted with broken line and the waveform computed using the following equation is plotted with gray line:

$$\begin{split} E_{z_\text{flat.tail}}\left(t\right) &= \frac{2}{\left(1 + \rho_{\text{bot}}\right)\left(1 - \rho_{\text{top}}\right)} \\ &\times \left[E_{z_\text{tall}}\left(t\right) - \rho_{\text{bot}}\rho_{\text{top}}E_{z_\text{tall}}\left(t - \frac{2h}{c}\right)\right]. \end{split} \tag{7}$$

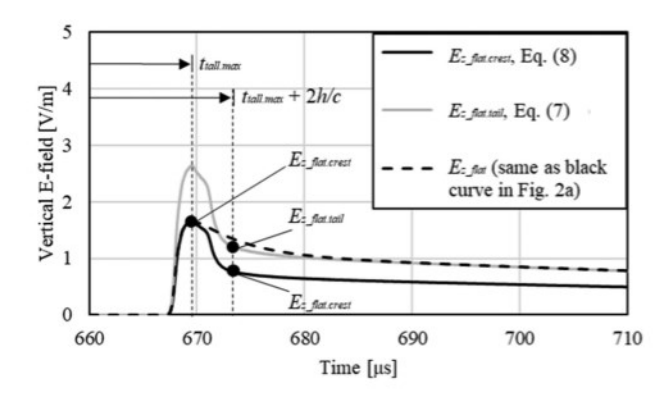


Fig. 3. Waveforms of electric field at 200 km due to a lightning strike to a 500-m tall object computed using (7) (gray line) and (8) (solid black line), and the waveform of electric field due to a lightning strike to flat ground (broken line).

While the tails of the gray-line and broken-line waveforms are similar, their peaks differ significantly. We can adjust the peak (crest) value using the following equation, but the agreement in the tail will be poor (see solid black line in Fig. 3):

$$E_{z_\text{flat.crest}}\left(t\right) = \frac{1}{k_{\text{tall}}} \left[E_{z_\text{tall}}\left(t\right) - \rho_{\text{bot}}\rho_{\text{top}}E_{z_\text{tall}}\left(t - \frac{2h}{c}\right) \right]$$

where the far-field enhancement factor k_{tall} , which is the ratio of the initial peaks of vertical electric field for the strike-object and flat-ground cases, is given by (3).

We can make the wavetail of electric field given by (8) (solid black line in Fig. 3) closer to that given by (7) (gray line in Fig. 3), by adding $\alpha^n E_{z_{\rm flat.crest}}(t)$ repeatedly for each 2h/c time increment to compensate for the difference, $E_{z_{\rm flat.tail}}(t_{\rm tall.max} + 2h/c) - E_{z_{\rm flat.crest}}(t_{\rm tall.max} + 2h/c)$ (see two vertically stacked black circles in Fig. 3). The resultant total electric field estimated for the corresponding lightning strike to flat ground is given as follows:

$$E_{z_{\rm flat.total}}\left(t\right) = \sum_{n=0}^{\infty} \frac{\alpha^n}{k_{\rm tall}} \begin{cases} E_{z_{\rm tall}}\left(t - \frac{2nh}{c}\right) \\ -\rho_{\rm bot}\rho_{\rm top}E_{z_{\rm tall}}\left(t - \frac{2(n+1)h}{c}\right) \end{cases}$$

where

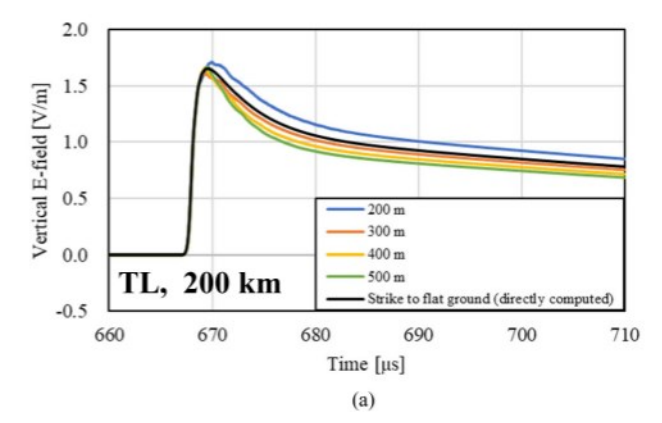
$$\alpha = \frac{E_{z_flat.tail}\left(t_{tall.max} + \frac{2h}{c}\right) - E_{z_flat.crest}\left(t_{tall.max} + \frac{2h}{c}\right)}{E_{z_flat.crest}\left(t_{tall.max}\right)}$$

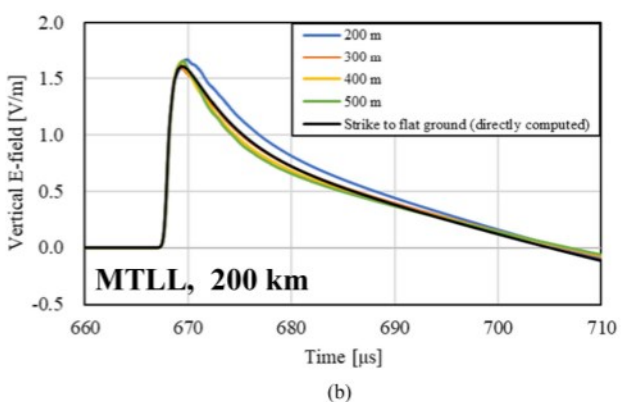
$$= \frac{1}{E_{z_flat.max}} \begin{bmatrix} \frac{2}{(1+\rho_{\rm bol})(1-\rho_{\rm lop})} & E_{z_flat.crest}\left(t_{\rm tall.max} + \frac{2h}{c}\right) \\ -\rho_{\rm bot}\rho_{\rm top}E_{z_tall}\left(t_{\rm tall.max}\right) \end{bmatrix} \\ -\frac{1}{k_{\rm tall}} & E_{z_tall}\left(t_{\rm tall.max} + \frac{2h}{c}\right) \\ -\rho_{\rm bot}\rho_{\rm top}E_{z_tall}\left(t_{\rm tall.max}\right) \end{bmatrix}$$

$$= \frac{1}{\frac{E_{z_tall.max}}{k_{\rm tall}}} \begin{bmatrix} \frac{1}{(1+\rho_{\rm bot})(1-\rho_{\rm top})} & E_{z_tall.min} - \rho_{\rm bot}\rho_{\rm top}E_{z_tall.max} \\ -\frac{1}{k_{\rm tall}} & E_{z_tall.min} - \rho_{\rm bot}\rho_{\rm top}E_{z_tall.max} \end{bmatrix}$$

$$= \begin{bmatrix} \frac{2k_{\rm tall}}{(1+\rho_{\rm bot})(1-\rho_{\rm top})} - 1 \end{bmatrix} \begin{pmatrix} \frac{E_{z_tall.min}}{E_{z_tall.max}} - \rho_{\rm bot}\rho_{\rm top} \end{pmatrix}$$

where n is zero or a positive integer [at n = 0 (9) reduces to (8)], $t_{\text{tall.max}}$ is the time at which the electric field due to a lightning strike to a tall object attains its first peak (see Fig. 3), $E_{z_{\text{-tall.max}}}$ is the first maximum value of the electric field, and





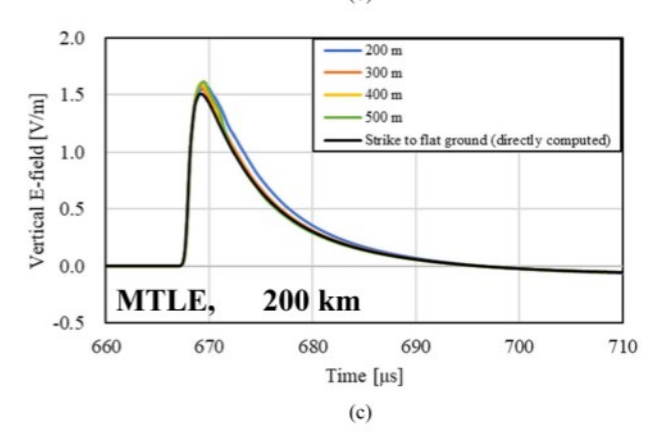


Fig. 4. Waveforms of electric field due to lightning strike to flat ground at a distance of 200 km from the lightning channel represented by (a) the TL model, (b) the MTLL model, and (c) the MTLE model, reconstructed from waveforms of electric field due to lightning strikes to 200, 300, 400, and 500-m tall objects. The waveform directly computed for the strike to flat ground is also shown.

 $E_{z_{\rm tall.min}}$ is the first minimum value of the electric field due to a lightning strike to a tall object (see Fig. 2 and Tables I–III), which appears around a time of 2h/c after the first-peak time. Note that, based on (8), the maximum value of the electric field due to the corresponding lightning strike to flat ground, $E_{z_{\rm flat.max}} = E_{z_{\rm flat.crest}}$ ($t_{\rm tall.max}$), is replaced by $E_{z_{\rm tall.max}}/k_{\rm tall}$.

Fig. 4 shows waveforms of electric field, due to the corresponding lightning strikes to flat ground at a distance of 200 km, reconstructed using (9) and (10) from the FDTD-computed waveforms of electric field due to lightning strikes to 200-, 300-, 400-, and 500-m tall objects. Also shown in Fig. 4 is the FDTD-computed waveform of electric field due to the same lightning

TL model

30

TL model

30

TL model

30

MTLL model

MTLE model

Original waveform

MTLL model

MTLE model

Original waveform

MTLL model

MTLE model

Original wave form

40

40

40

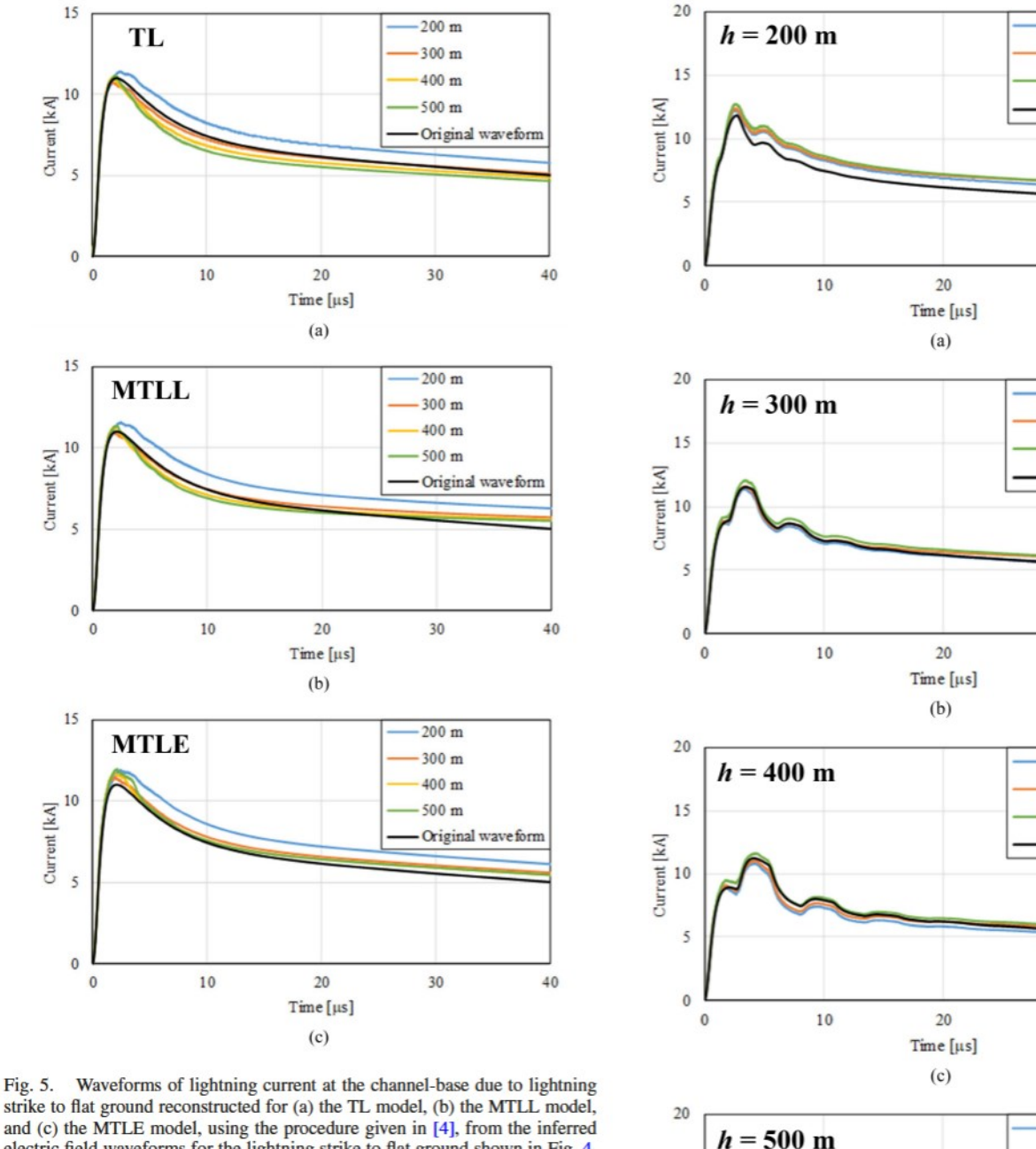


Fig. 5. Waveforms of lightning current at the channel-base due to lightning strike to flat ground reconstructed for (a) the TL model, (b) the MTLL model, and (c) the MTLE model, using the procedure given in [4], from the inferred electric field waveforms for the lightning strike to flat ground shown in Fig. 4. The original channel-base current waveform (used as input in computing fields due to strikes to flat ground) is also shown: $I(0, t) = (1 + \rho_{\rm gr})I_{\rm sc}$ (0, t)/2. The inferred channel-base current waveforms were converted to $I_{\rm sc}$ according to (2), $I_{\rm sc}(0, t) = 2I(0, t)/(1 + \rho_{\rm gr})$, and used in computing the strike-object current waveforms predicted by the TL, MTLL, and MTLE models and shown in Figs. 6 and 7.

strike but terminated on to flat ground. It appears from Fig. 4 that (9) allows one to reasonably well reconstruct the electric field waveform due to the corresponding lightning strike flat ground from those due to lightning strikes to tall objects. Quantities needed are the height of tall but terminated on object, current reflection coefficients at the top and bottom of the tall object (or the equivalent impedance of lightning channel, the characteristic impedance of tall object, and the grounding impedance), and the speed of current wave propagating along the channel.

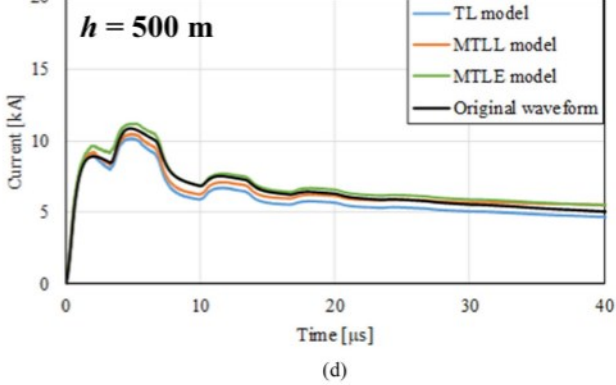


Fig. 6. Waveforms of lightning current at the top of the strike object of height (a) h = 200 m, (b) h = 300 m, (c) h = 400 m, and (d) h = 500 m, reconstructed from waveforms of electric field at a distance of 200 km, using the procedure proposed in this paper. Also shown are the "original" current waveforms, directly computed using (1a).

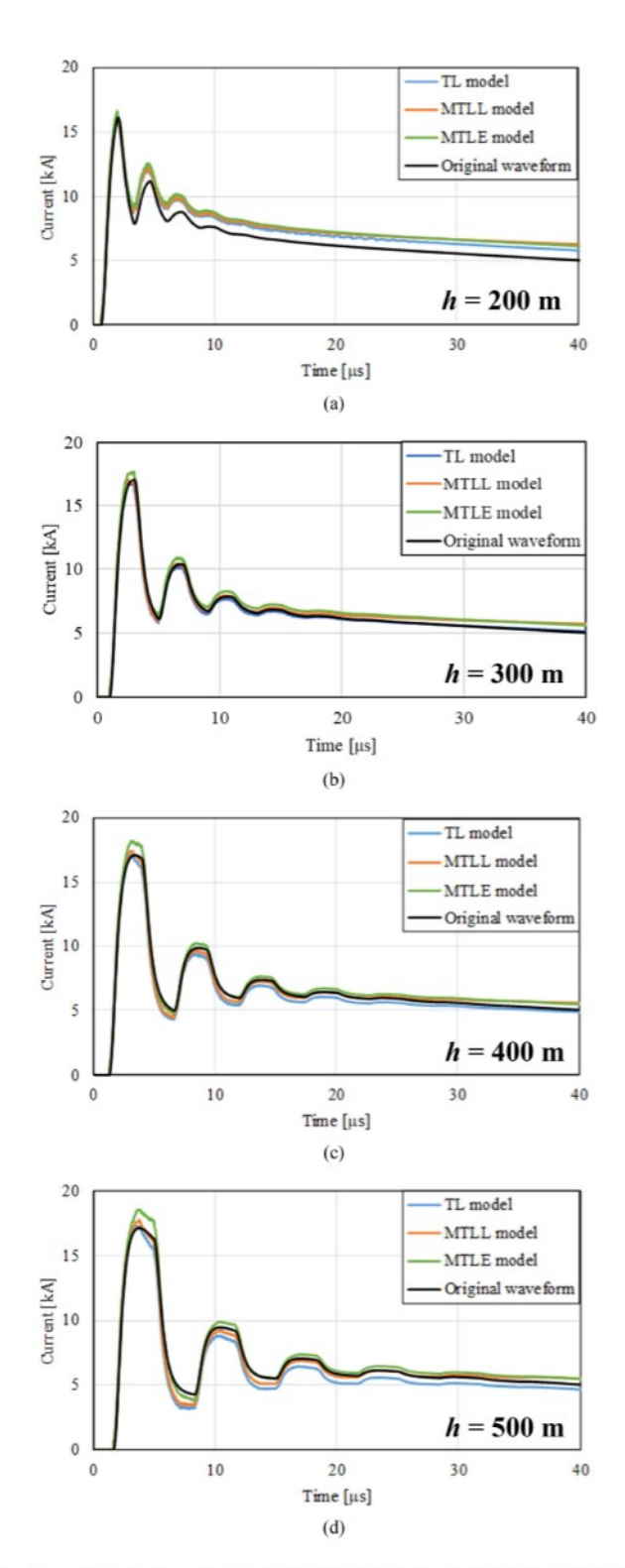


Fig. 7. Same as Fig. 6, but at the bottom of the strike object of height (a) h = 200 m, (b) h = 300 m, (c) h = 400 m, and (d) h = 500 m.

V. RECONSTRUCTION OF CHANNEL-BASE CURRENT WAVEFORM FROM ELECTRIC-FIELD WAVEFORM FOR LIGHTNING STRIKE TO FLAT GROUND

Expressions for reconstructing the channel-base current waveform from vertical electric-field waveform on perfectly conducting ground have been derived for the MTLL and MTLE return-stroke models in [4]. Fig. 5 shows waveforms of channel-base current, which are reconstructed from the electric field waveforms for the lightning strike to flat ground in the preceding section and shown in Fig. 4.

The waveform of current at any altitude along the strike object (if any) and the lightning channel can be calculated using (1a), (1b), and (2) if the waveform of short-circuit current $I_{\rm sc}$ is specified. Fig. 6 shows waveforms of lightning current at the top of the object, due to a lightning strike to a 200-, 300-, 400-, or 500-m tall object, computed using (1a) and inferred channel-base current waveforms I(0, t) shown in Fig. 5 [which are converted to $I_{\rm sc}$ according to (2): $I_{\rm sc}(0, t) = 2I(0, t)/(1+\rho_{\rm gr})$]. Fig. 7 is similar to Fig. 6, but for the current at the bottom of the strike object. It appears from Figs. 6 and 7 that the proposed procedure allows one to reconstruct the current waveform at any height along the strike object.

VI. SUMMARY

In this article, we have proposed a procedure to reconstruct the waveform of far electric field due to the lightning strike to flat ground from the corresponding waveform of far electric field due to a lightning strike to a tall object. Then, we have estimated the waveform of channel-base current for the strike to flat ground using the procedure proposed by Fukuyama et al. [4]. Further, we have demonstrated how the waveform of current at any height along the strike object and the lightning channel can be inferred using the expressions proposed by Baba and Rakov [13]. Computations of far electric fields due to lightning strikes to tall objects were carried out using the FDTD method. The lightning return stroke was represented by the widely used TL, MTLL, and MTLE models.

APPENDIX: TIME-UPDATE EQUATIONS OF ELECTRIC AND MAGNETIC FIELDS FOR THE FDTD METHOD IN THE 2-D CYLINDRICAL COORDINATE SYSTEM

In analyzing electromagnetic field pulses, which are radiated from a vertical lightning channel and propagate over an azimuthally symmetric ground, it is advantageous to use the 2-D cylindrical coordinate system since it requires less computation time and memory than the 3-D Cartesian coordinate system. In the 2-D cylindrical coordinate system, there exist only the radial and vertical components of electric field, E_T and E_Z , respectively, and the azimuthal component of magnetic field, H_{φ} . The FDTD method in this coordinate system requires the 2-D working space to be divided into square or rectangular cells. Time-update equations for E_T and E_Z , are derived from Ampere's law, and that for H_{φ} is derived from Faraday's law.

Update equations for E_r at a location (i+1/2, j) and E_z at a location (i, j+1/2) (see Fig. 8) are given as follows [15]:

$$E_r^n\left(i + \frac{1}{2}, j\right) = \frac{1 - \frac{\sigma(i+1/2, j)\Delta t}{2\varepsilon(i+1/2, j)}}{1 + \frac{\sigma(i+1/2, j)\Delta t}{2\varepsilon(i+1/2, j)}} E_r^{n-1}\left(i + \frac{1}{2}, j\right) + \frac{\frac{\Delta t}{\varepsilon(i+1/2, j)}}{1 + \frac{\sigma(i+1/2, j)\Delta t}{2\varepsilon(i+1/2, j)}} \frac{1}{\Delta z} \begin{bmatrix} -H_{\varphi}^{n-\frac{1}{2}}\left(i + \frac{1}{2}, j + \frac{1}{2}\right) \\ +H_{\varphi}^{n-\frac{1}{2}}\left(i + \frac{1}{2}, j - \frac{1}{2}\right) \end{bmatrix}$$

$$(11)$$

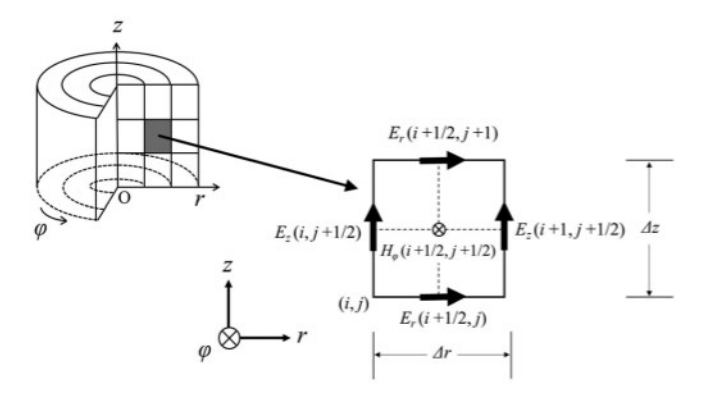


Fig. 8. Placement of radial E_r and vertical E_z components of electric field and azimuthal component of magnetic field H_φ in a cell in the 2-D cylindrical coordinate system.

$$\begin{split} E_z^n\left(i,j+\frac{1}{2}\right) &= \frac{1 - \frac{\sigma(i,j+1/2)\Delta t}{2\varepsilon(i,j+1/2)}}{1 + \frac{\sigma(i,j+1/2)\Delta t}{2\varepsilon(i,j+1/2)}} \ E_z^{n-1}\left(i,j+\frac{1}{2}\right) \\ &+ \frac{\frac{\Delta t}{\varepsilon(i,j+1/2)}}{1 + \frac{\sigma(i,j+1/2)\Delta t}{2\varepsilon(i,j+1/2)}} \frac{1}{r_i\Delta r} \begin{bmatrix} r_{i+1/2}H_\varphi^{n-\frac{1}{2}}\left(i+\frac{1}{2},j+\frac{1}{2}\right) \\ -r_{i-1/2}H_\varphi^{n-\frac{1}{2}}\left(i-\frac{1}{2},j+\frac{1}{2}\right) \end{bmatrix} \end{split}$$
(12)

where r_i is the radial distance from the z-axis to the location of $E_z(i,j+1/2), r_{i-1/2}$ is the distance from the z-axis to the location of H_{φ} $(i-1/2,j+1/2), r_{i+1/2}$ is the distance from the z-axis to the location of H_{φ} $(i+1/2,j+1/2), \Delta r$ is the cell side length in the radial direction, and Δz is the cell side length in the vertical direction.

The update equation for $H_{\varphi}^{n+1/2}$ at a location (i+1/2, j+1/2) (see Fig. 8) is given as follows [14]:

$$\begin{split} H_{\varphi}^{n+\frac{1}{2}}\left(i+\frac{1}{2},j+\frac{1}{2}\right) &= H_{\varphi}^{n-\frac{1}{2}}\left(i+\frac{1}{2},j+\frac{1}{2}\right) \\ &-\frac{\Delta t}{\mu(i+1/2,j+1/2)}\frac{1}{\Delta z}\left[E_{r}^{n}\left(i+\frac{1}{2},j+1\right)-E_{r}^{n}\left(i+\frac{1}{2},j\right)\right] \\ &+\frac{\Delta t}{\mu(i+1/2,j+1/2)}\frac{1}{\Delta r}\left[E_{z}^{n}\left(i+1,j+\frac{1}{2}\right)-E_{z}^{n}\left(i,j+\frac{1}{2}\right)\right]. \end{split} \tag{13}$$

By updating E_r^n, E_z^n , and $H_\varphi^{n+1/2}$ at every point in the working space, transient electric and magnetic fields throughout the working space are obtained.

A current source $I_z^{n-1/2}$ at point (0, j+1/2) along the z-axis in the 2-D cylindrical coordinate system is represented by specifying the circulating magnetic field closest to the source, with the corresponding update equation being as follows [15]:

$$H_{\varphi}^{n-\frac{1}{2}}\left(\frac{1}{2}, j+\frac{1}{2}\right) = \frac{1}{2\pi\left(\frac{\Delta r}{2}\right)} I_z^{n-\frac{1}{2}}\left(0, j+\frac{1}{2}\right).$$
 (14)

REFERENCES

- A. J. Eriksson, "Lightning and tall structures," Trans. South Afr. IEE, vol. 69, pp. 238–252, 1978.
- [2] V. A. Rakov, "Transient response of a tall object to lightning," *IEEE Trans. Electromagn. Compat.*, vol. 43, no. 4, pp. 654–661, Nov. 2001.
- [3] F. Rachidi, "Modeling lightning return strokes to tall structures: A review," J. Lightning Res., vol. 1, pp. 16–31, 2007.
- [4] M. Fukuyama, S. Koike, Y. Baba, T. Tsuboi, and V. A. Rakov, "Reconstruction of channel base current waveforms from electromagnetic field waveforms degraded by propagation effects," in *Proc. 35th Int. Conf. Lightning Protection XVI Int. Symp. Lightning Protection*, Sep. 2021, pp. 1–6.

- [5] Y. Baba and V. A. Rakov, "On the use of lumped sources in lightning return stroke models," J. Geophys. Res., vol. 110, no. D3, 2005, Art. no. D03101, doi: 10.1029/2004JD005202.
- [6] K. S. Yee, "Numerical solution of initial boundary value problems involving Maxwell's equations in isotropic media," *IEEE Trans. Antennas Propag.*, vol. 14, no. 3, pp. 302–307, May 1966.
- [7] M. A. Uman, D. K. Mclain, and E. P. Krider, "The electromagnetic radiation from a finite antenna," *Amer. J. Phys.*, vol. 43, pp. 33–38, 1975.
- [8] V. A. Rakov and A. A. Dulzon, "Calculated electromagnetic fields of lightning return stroke," *Tekhnicheskaya Elektrodinamika*, vol. 1, pp. 87–89, 1987.
- [9] C. A. Nucci, C. Mazzetti, F. Rachidi, and M. Ianoz, "On lightning return stroke models for LEMP calculation," in *Proc. 19th Int. Conf. Lightning Protection*, 1988, pp. 463–470.
- [10] Z. P. Liao, H. L. Wong, B. P. Yung, and Y. F. Yuan, "A transmitting boundary for transient wave analysis," Sci. China, Ser. A, vol. 27, no. 10, pp. 1063–1076, 1984.
- [11] Y. Baba and V. A. Rakov, "On the transmission line model for lightning return stroke representation," *Geophys. Res. Lett.*, vol. 30, no. 24, pp. 1–4, Dec. 2003, doi: 10.1029/2003GL018407.
- [12] F. Heidler, "Traveling current source model for LEMP calculation," in Proc. 6th Int. Zurich Symp. Electromagn. Compat., 1985, pp. 157–162.
- [13] Y. Baba and V. A. Rakov, "Lightning EM environment in the presence of a tall, grounded strike object," J. Geophys. Res., vol. 110, no. D9, 2005, Art. no. D09108, doi: 10.1029/2004JD5505.
- [14] Y. Baba and V. A. Rakov, "Lightning strikes to tall objects: Currents inferred from far electromagnetic fields versus directly measured currents," *Geophys. Res. Lett.*, vol. 34, 2007, Art. no. L19810, doi: 10.1029/2007GL030870.
- [15] Y. Baba and V. A. Rakov, Lightning-Induced Effects in Electrical and Telecommunication Systems. London, U.K.: Institute of Engineering and Technology, 2020, p. 243.



Shunsuke Koike received the B.Sc. degree in electrical engineering from the Doshisha University, Kyoto, Japan, in 2021.

Since 2021, he has been a Graduate Student with the same University. His research interest includes computational electromagnetics.



Yoshihiro Baba (Fellow, IEEE) received the B.Sc., M.Sc., and Ph.D. degrees in electrical engineering from the University of Tokyo, Tokyo, Japan, in 1994, 1996, and 1999, respectively.

He has been a Professor with the Doshisha University, Kyoto, Japan, since 2012, and the Dean of the Institute of Advanced Research and Education, Doshisha University, since 2022. From 2003 to 2004, he was a Visiting Scholar with the University of Florida, Gainesville, FL, USA. He has authored or coauthored of 4 books, 7 book chapters, and more

than 130 papers published in reviewed international journals.

Prof. Baba was the recipient of the Technical Achievement Award from the IEEE EMC Society in 2014. He was an Editor of the IEEE TRANSACTIONS ON POWER DELIVERY from 2009 to 2018, a Guest Associate Editor of the IEEE TRANSACTIONS ON ELECTROMAGNETIC COMPATIBILITY from 2018 to 2019, and an Associate Editor of Electrical Engineering (Springer Journal) from 2019 to 2022. He was the Convener of C4.37 Working Group of the International Council on Large Electric Systems from 2014 to 2019, and a Vice President of the Power and Energy Society of the Institute of Electrical Engineers of Japan (IEEJ) from 2020 to 2022. He has been the Vice Chairperson of the Steering Committee of the Asia-Pacific International Conference on Lightning since 2017, and an Associate Editor of the IEEE TRANSACTIONS ON ELECTROMAGNETIC COMPATIBILITY since 2022. He is a Fellow of the Institution of Engineering and Technology and of the IEEJ.



Toshihiro Tsuboi received the B.Sc. and M.Sc. degrees in electrical engineering from the Tokyo Institute of Technology, Tokyo, Japan, in 1997 and 1999, respectively, and the Ph.D. degree in electrical engineering from the Chiba University, Chiba, Japan, in 2013.

He joined the Tokyo Electric Power Company, Tokyo, Japan, in 1999, and is currently a Senior Researcher with the Tokyo Electric Power Company Research Institute, Yokohama, Japan. Since 2020, he has been an Adjunct Professor with the Doshisha

University, Kyoto, Japan. His research interest includes insulation design of power systems.



Vladimir A. Rakov (Fellow, IEEE) received the M.S. and Ph.D. degrees in electrical engineering from the Tomsk Polytechnical University (Tomsk Polytechnic), Tomsk, Russia, in 1977 and 1983, respectively.

From 1977 to 1979, he was an Assistant Professor of electrical engineering with the Tomsk Polytechnic. In 1978, he joined the Lightning Research Group, High Voltage Research Institute (a division of Tomsk Polytechnic), where from 1984 to 1994, he held the position of the Director of the Lightning Research Laboratory. He is currently a Distinguished Professor

with the Department of Electrical and Computer Engineering, University of Florida, Gainesville, FL, USA, and a Director of the International Center for Lightning Research and Testing. He as authored or coauthored 5 books, and more than 800 other publications on various aspects of lightning, with more than 300 papers being published in reviewed journals.

Prof. Rakov is a Fellow of the American Geophysical Union, the American Meteorological Society, and the Institution of Engineering and Technology.